Eur Arch Psychiatry Clin Neurosci (1998) 248 : 161–170

ORIGINAL PAPER

Frank Häger · Hans-Peter Volz · Christian Gaser
Hans-Joachim Mentzel · Werner A. Kaiser
Heinrich Sauer

Challenging the anterior attentional system with a continuous performance task: a functional magnetic resonance imaging approach

Received: 18 September 1997 / Accepted: 9 March 1998

Abstract Combining the Continuous Performance Test (CPT) with a modern functional imaging technique provides a powerful tool for investigating neurophysiological processes in the human brain. There is increasing evidence from single photon emission tomography (SPECT), positron emission tomography (PET) and presently also functional magnetic resonance imaging (fMRI) studies proposing the existence of a distributed large-scale attentional network, mediated by the dorsolateral prefrontal and mesial frontal cortex, thalamus, basal ganglia and posterior parietal and superior temporal lobe. The aim of this study is to show that fMRI is a useful tool for in vivo localization of attentional tasks and to compare the results with established imaging techniques. Functional MRI was performed on a clinical 1.5-T system using gradient-echo acquisition. For data processing, the Statistical Parametric Mapping (SPM96) package was used. A right lateralized activation pattern in the dorsolateral prefrontal and mesial frontal cortex, the thalamus and the basal ganglia was found in a group of 12 male subjects. These findings support theories suggesting right hemispheric dominance of human attention.

Key words Continuous Performance Test · Functional MRI · Brain imaging · Cognitive stimulation

Introduction

Attention is a complex process or a set of processes. Lesion studies suggest that the most common sensory-perceptual disorders in brain-damaged patients are caused by abnormalities of attention (for a recent review see Heilman et al. 1994). Mirsky et al. (1991) presented a neuropsychological model, mainly based on lesion studies, for conceptualizing the components or elements of attention. The model replaces the diffuse and global concept of "attention" by a group of four processes (focus-execute, sustain, shift and encode) and links them to a putative system of cerebral structures.

The element of attention that Mirsky et al. (1991) named "*sustain*" is particularly dependent on brain-stem and thalamic portions of the attentional system. The inferior parietal cortex, the superior temporal gyrus and the caudate nucleus are parts of the brain system involved in the *focus-execute* element of attention. The medial frontal cortex, the dorsolateral prefrontal regions and the anterior cingulate gyrus are included in the focal representation of the *shift* element. The *encode* element is related to the hippocampus and amygdala.

In addition to the classic approach of linking neuropsychological data to lesion studies, further evidence for the involvement of distinct brain structures for attention processing arose from functional imaging procedures positron emission tomography (PET), single photon emission tomography (SPECT) and functional magnetic resonance imaging (fMRI), mostly comparing schizophrenic subjects with normal controls.

These studies suggest that challenging the brain with an attention-demanding task increases the activity of a large-scale neuronal network in normal subjects. A widely used neuropsychological task for assessing vigilance and sustained attention is the Continuous Performance Test (CPT; Rosvold et al. 1956; Nestor et al. 1991; Nuechterlein 1991). Despite its low sensitivity and specificity, this simple cognitive task is a useful instrument for functional imaging studies (Weintraub and Mesulam 1985).

The results of SPECT (Berman et al. 1986; Rezai et al. 1993; Keilp et al. 1997), PET (Cohen et al. 1987; Cohen et al. 1988; Buchsbaum et al. 1990; Buchsbaum et al. 1992; Siegel et al. 1992; Siegel et al. 1993; Schroeder et al. 1994; Siegel et al. 1995) and fMRI (Cohen and Servan-Schreiber 1994; Breiter 1995; Pugh et al. 1996) including

F. Häger (✉) · H.-P. Volz · C. Gaser · H. Sauer
Department of Psychiatry, Hans-Berger-Kliniken,
University of Jena, Philosophenweg 3, D-07740 Jena, Germany

H.-J. Mentzel · W. A. Kaiser
Institute of Diagnostic and Interventional Radiology,
Hans-Berger-Kliniken, University of Jena, Philosophenweg 3,
D-07740 Jena, Germany

visual or auditory versions of the CPT similar to the version used in the current study are inconsistent. By means of different techniques, these authors found elevated metabolic rates in the right middle prefrontal cortex, partially in combination with decreased rates in the anterior cingulum (Cohen et al. 1988). Furthermore, higher metabolic rates in the right frontal and temporoparietal region (Buchsbaum et al. 1990), as well as significantly increased blood flow in the left and, to a lesser extent, in the right mesial frontal cortex (Rezai et al. 1993) have been observed. Siegel et al. (1995) found a positive correlation between performance and glucose metabolism in the medial superior frontal and lateral inferior temporal gyri. Not all studies examining frontal lobe function during CPT performance yielded positive results. Berman et al. (1986) reported the absence of any correlation between CPT performance and prefrontal activation in either schizophrenics or normal controls.

Whereas other studies used sets of tasks that vary demands on attention, we intended to measure the actual attentional level while performing the task in the scanner system. We chose a slice orientation that covers most of the regions proposed to be involved in attention, except for the posterior parietal cortex.

The purpose of the present investigation was to answer the following questions: (a) Is fMRI able to detect attention related activation in areas proposed to be involved in an attention-related system? (b) Is brain activation dependent on task performance?

Subjects and methods

Fourteen healthy male volunteers were recruited by public advertisement. Of these, 12 subjects (mean age 27.9 years, SD 6.4 years, range 20–41 years) were included in the present study. All probands were right-handed, unmedicated and had no history of psychiatric disorders; none had first-degree relatives with a psychiatric illness. All volunteers were native German speakers and were not paid for their participation.

The participants were screened thoroughly for internal and neurological symptoms; persons exhibiting such symptoms or with first-degree relatives showing severe neurological disorders were excluded. A history or presence of alcohol or substance abuse was a further exclusion criterion. A complete set of 3D MR images were acquired to exclude gross morphological abnormalities.

Written informed consent was obtained from all volunteers after the scanning and test procedure had been explained. The study was approved by the ethical review board of the University of Jena.

Scanning and test procedures

Imaging was performed with a conventional MRI scanner at 1.5 T (Philips Gyroscan ACSII Philips, Best, The Netherlands) using a standard head coil. For functional imaging, a T2*-weighted gradient-echo sequence was used: echo time (TE) 50 ms, repetition time (TR) 100 ms, flip angle 40 °C, field of view (FOV) 23 cm, matrix 256 × 256, slice thickness 10 mm. Scanning also included acquisition of three high-resolution anatomical images. These images were localized at the same plane and centre position as the T2*-weighted images, using a T1-weighted sequence with TE 15 ms, TR 300 ms, FOV 23 cm, matrix 256 × 256 and a slice thickness of 3 mm.

Since we were restricted to single-slice functional imaging, an orientation matching the following criteria was selected: inclusion of the cross section of regions of interest presumably involved in the above-mentioned attention processes, low susceptibility artefacts, reliable and fast planning procedure. An extensive planning procedure guaranteed maximal reliability of the orientation and location of imaging planes across test sessions and subjects. The aim of this procedure was to obtain images with the same position and direction in the Talairach space. The anterior and posterior commissures (CA, CP) were identified, and the CA–CP line and the vertical to the CA–CP in CA (VCA) line (according to Talairach and Tournoux 1988) were used as navigational markers. Images were obtained in a slice parallel to the line between the posterior and superior top of the CA–CP and VCA line, respectively, passing through CP (see Fig. 1).

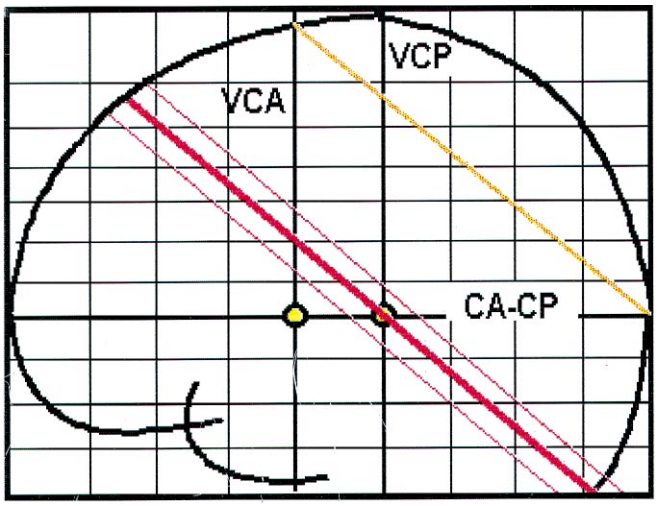

Fig. 1 Slice planning, T_1-weighted (echo time: 15 ms; repetition time: 300 ms; field of view: 230 mm; matrix 256 × 256; slice thickness: 10 mm) *CA–CP* line passing Commissura anterior (CA) and Commissura posterior (CP); *VCA* vertical line to the CA–CP line crossing the line in CA

Because the study was designed to find group differences, we measured with 10-mm slice thickness. This equals an additional smoothing and minimizes the anatomical variability and the inevitable pitfalls of the used single-slice technique, based on uncorrected pitch and role movements.

Stimulation

The various versions of the CPT typically involve tachistoscopic presentations (40–200 ms) of a pseudorandom series of letters or numerical stimuli at a rapid, fixed rate with the instruction to respond to a predetermined stimulus. In the used CPT-double-T, a target consists of the consecutive recurrence of the letter T. To decide whether or not the current T is a target, contextual information provided by the previous stimulus is required.

For stimulation in the scanner, we used the STIM-PC version (Neuroscan 1990) of the CPT-double-T, transformed by the matrix 1000-device (I-DEN Corporation, San Diego, USA). The material was projected via a Philips LC 2000 projector (Philips, Best, The Netherlands) on a rear screen placed in front of the scanner. By means of an angled mirror placed above the head coil, the screen was visible for the participant. Subjects were asked to press a hydropneumatic response device as fast as possible when a T was followed by another T. Each stimulus block consisted of 36 targets, 18 distractors and 126 nontargets presented in pseudorandom order. Target probability was 25%, the interstimulus interval 1.2 s and stimulus exposure time 0.6 s. All subjects performed the task four times. Test performance was assessed on-line using the STIM-protocol. On the day before fMRI measurement, a learning session of 15 min took place during which the subjects were accustomed to the test procedure.

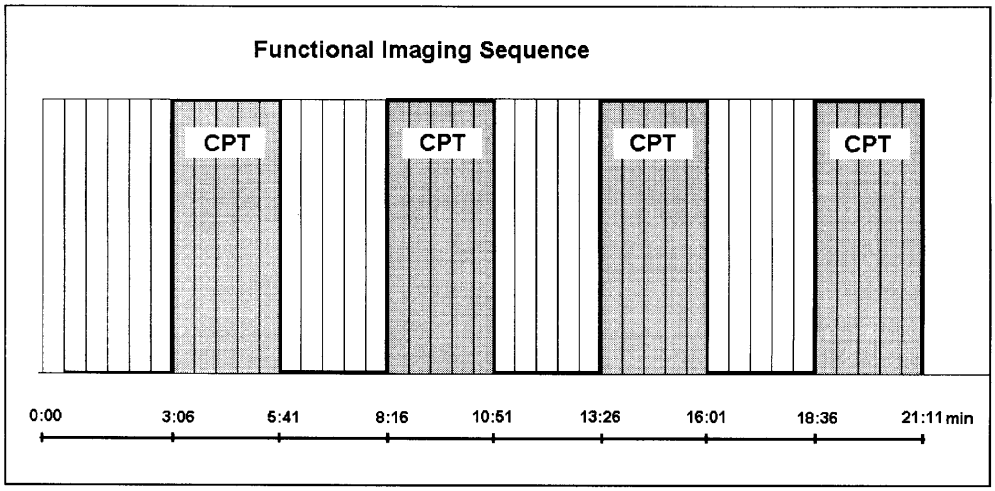

Fig. 2 Stimulus sequence for data acquisition

Table 1 Continuous Performance Test: performance data (*A:* good; *B:* poor; *total* whole group, *d'* sensitivity, *ln β* ln of likelihood criterion)

	A		B		Total	
Mean age	27	(4.8)	29	(8.8)	28	(6.5)
Correct responses (%)	99.5	(0.79)	95.4	(3.47)	97.09	(3.37)
Response time (s)	0.39	(0.07)	0.39	(0.1)	0.39	(0.08)
Ommission errors	0.44	(0.6)	3.58	(5.8)	2.27	(4.59)
Commission errors	0		2.47	(1.91)	1.44	(1.90)
Hit rate	0.98	(0.03)	0.85	(0.16)	0.90	(0.14)
False-alarm rate	0		0.02	(0.01)	0.01	(0.01)
d′	5.16	(0.23)	3.57	(0.72)	4.24	(0.99)
In β	3.27	(0.37)	1.89	(1.57)	2.47	(1.38)
Motion (*x*-axis; mm)	0.33	(0.15)	0.39	(0.2)	0.36	(0.18)
Motion (*y*-axis; mm)	0.57	(0.18)	0.55	(0.34)	0.56	(0.27)
Rotation (°)	0.32	(0.11)	0.4	(0.12)	0.37	(0.12)

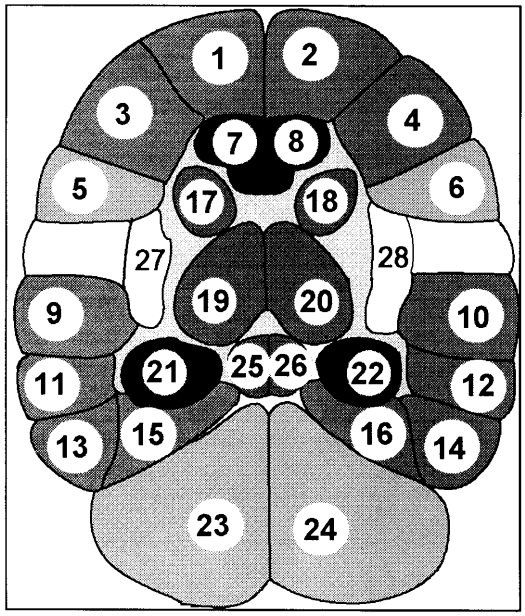

Fig. 3 Regions of interest (ROIs) overlaid on the averaged anatomical slice. *1, 2* Prefrontal cortex, superior gyrus; *3–6* prefrontal cortex, dorsolateral part; *7, 8* anterior cingulate ; *9, 10* temporal lobe (gyrus temporalis superior); *11–14* temporal lobe (gyrus temporalis medialis and inferior); *15, 16* temporal lobe (fusiform gyrus); *17, 18* caudatus; *19, 20* thalamus; *21, 22* hippocampus; *23, 24* cerebellum; *25, 26* midbrain (superior colliculus)

During measurement, the ears were plugged with wax to reduce the noise level in the scanner. In a so-called baseline condition, subjects were asked to count silently, eyes opened, while pushing down the buttons of the response device in a freely chosen rhythm. Subjects were instructed to watch the screen carefully, because the starting of the test was not otherwise signaled.

Each series began with one image at rest (31 s) allowing MRI signal equilibrium to be reached, followed by 40 images alternating baseline condition and activation every 2 min, 35 s (5 min, 10 s per cycle, ten images per cycle, four cycles). The whole procedure took approximately 30 min (see Fig. 2).

Performance on the CPT can be evaluated in various ways. We chose errors of omission and commission (hit rate and false-alarm rate) as well as mean response time. Since it was our aim to determine the actual behaviour while performing the task as precisely as possible, we evaluated d' (discriminability or sensitivity) and β (response criterion), derived from signal detection theory (Pollack and Norman 1964; Grier 1971; Egan 1980; Nuechterlein 1991), in addition to the traditional measures. The signal detection index d', sensitivity, has been used in experimental psychology to identify the ability to discriminate target and nontarget stimuli. The index d' is obtained by calculating the hit rate and false-alarm rate, finding their normal deviates, and then subtracting the normal deviate of the hit rate from that of the false-alarm rate. The d' index represents the distance between the means of the signal and noise distributions in standard deviation units. To find β, the corresponding index of response criterion, the ordinates of the normal distribution for the hit rate and false-alarm rate must be found. The ratio of the ordinate of the hit rate to that of the false-alarm rate equals β. The natural log of β, or lnβ, is typically used for statistical calculations to produce distributions that represent the amount of change in response criterion in a more linear fashion.

A subject with a high sensitivity has a relatively high hit rate (i.e. few errors of omission) and a relatively low false-alarm rate (few errors of commission). The response criterion β measures the amount of perceptual evidence that the subject requires to decide that a stimulus is a target. A subject with a 'cautious' response criterion has a low target hit rate and a low false-alarm rate in contrast to more 'liberal subjects'. Using ln β and d', we divided the subjects into good and poor performers (group A and group B, respectively).

Image analysis

The fMRI data were analysed with statistical parametric mapping software SPM96 (Friston 1996) implemented in MATLAB. SPM96 combines the general linear model and the theory of Gaussian fields. Set level inferences represent a new way of assigning *P*-values to distributed effects (Friston et al. 1996). Set level inference refers to the statistical inference that the number of clusters (defined by a height threshold and extent threshold) comprising an observed activation profile is highly unlikely to have occurred by chance. Because there is only one excursion set, there is no multiple comparison problem at this level of inference.

In order to remove the effects of head movements, the scans of each subject were first realigned. The realignment of subsequent slices in a time series used a least-squares approach to the first scan as a reference. The motion was corrected using three parameters: translation x, translation y and rotation α. The 12 subjects were controlled for the amount of motion. These data are given in Table 1.

Following realignment, all images were transformed into a standard space (Talairach and Tournoux 1988; Friston 1996) using 2D affine transformation and then smoothed with a 4-mm full width at half maximum (FWHM) isotropic kernel to match lattice assumptions made by the SPM program. For group analysis, the realigned images were smoothed with a 6-mm FWHM Gaussian kernel.

The design matrix was specified, including global activity as a confounding covariate. For single-subject analysis we used a simple subtractive design (on vs off). Differences in activation between good and poor performers were assessed by means of a factorial design with a group vs condition interaction.

We computed both the on–off and off–on contrast. The latter refers to the case in which the signal intensity in the resting condition exceeds the intensity for the active condition. The resulting SPM{Z} were thresholded at $P = 0.05$ for height (u) and uncorrected $P = 0.5$ for the spatial extent (k). For the on–off contrast the SPM{Z} maps were overlaid on the corresponding anatomical slices using a red colour scale, and for the off–on contrast we used a blue scale.

The anatomical boundaries (see Fig. 3) were determined manually before data analysis.

Results

Two of the 14 healthy male subjects recruited showed head movements of more than 2° and were therefore rejected. Using β and d' we divided the subjects into good (group A) and poor performers (group B). The cutoff values for group A were $\ln \beta > 2$ and $d' > 3.5$ (see Table 1).

Artefact detection

The mean motion correction per image was 0.36 mm (SD: 0.18 mm) in the x-direction, 0.56 mm (SD: 0.27 mm) in

Table 2 Data characterize the activation profile in terms of set level inference, or *P*-value, based on the number of clusters, c. For each cluster, a *P*-value reflects the cluster-level interference based on the number of voxels comprising the cluster k, and *P*-values corresponding to voxel-level inferences based on the z-score of selected maxima within each cluster. The uncorrected *P*-values and location (x, y, z mm) of these voxels are also provided. The footnotes specify the thresholds used and the parameters that relate to this particular analysis

	BA	ROI	Cluster level	k	Z	Voxel-level	Z	Uncorrected	k and Z	x	y	z
Positive activations one-sided *t*-test (on-off) set level 0.277 (6)												
Talamus dex.		19	0.003	594	6.5	0.000	6.50	0.000	0.000	1	–12	8
Thalamus sin.		20				0.001	4.76	0.001	0.000	–9	–7	11
Nc. caudatus dex.		17				0.001	4.72		0.000	17	11	23
DLPFC dex.	BA 9	3	0.017	557	5.44	0.000	5.44	0.000	0.000	30	43	44
DLPFC dex.	BA 9	5				0.023	4.05		0.000	41	38	41
DLPFC dex.	BA 45	3				0.758	2.71		0.003	37	27	33
Cing. ant. dex.	BA 24 (32)	7	0.021	372	5.08	0.000	5.08	0.005	0.000	8	26	33
Mesial prefront dex.	BA 8	1				0.027	4.00		0.000	3	45	45
Cing. ant. dex.	BA 33 (24)	7				0.726	2.75		0.003	9	17	27
Gyr. temp. sup. dex. (prof.)	BA 22	9	0.051	55	4.5	0.004	4.50	0.455	0.000	47	–30	–4
DLPFC sin.	BA 9	4	0.095	67	4.12	0.017	4.12	0.383	0.000	–35	40	42
						0.089	3.66		0.000	–27	44	45
Gyr. temp. sup. dex. (sup.)	BA 22	9	0.196	70	3.71	0.076	3.71	0.367	0.000	60	–28	–3
Negative activations one-sided *t*-test (off-on) set level 0.437 (5)												
Insula post. dex.		27	0.041	67	4.64	0.002	4.64	0.388	0.000	40	–17	4
Insula post. sin.		28	0.06	69	4.39	0.006	4.39	0.378	0.000	–39	–21	2
Hippocampus sin.		22	0.213	221	3.66	0.089	3.66	0.044	0.000	–26	–46	–15
Hippocampus sin.		22				0.245	3.31		0.000	–26	–46	–15
						0.290	3.25		0.011	–15	–42	–12
Hippocampus dex.		21	0.237	127	3.6	0.108	3.60	0.167	0.000	13	–39	–10
Pulvinar sin.		19				0.969	2.28		0.011	15	–27	–2
Gyr. temp. sup. sin. (supl.)	BA 41	10	0.989	51	1.93	0.998	1.93	0.487	0.027	–46	–11	8

Height threshold {u}= 1.64, $p = 0.05$; extent threshold {k} = 49.1 (48.4) voxels, $p = 0.5$; expected voxels per cluster, E{n} = 70.9 (69.8); expected number of clusters, E{m} = 4.3 (4.4); volume {S} = 12302 (12250) voxels; degree of freedom due to error = 455.0; smoothness FWHM {mm } = 8.7 9.9 {voxels} = 9.6 11.0 (10.8)

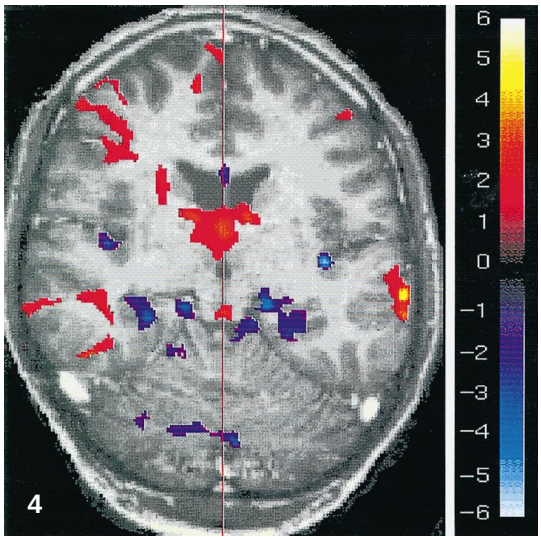

Fig. 4 Single-experiment result (male, 23 years, g16). T_2*-weighed gradient-echo sequence (FFE): TE 50 ms, TR 100 ms, field of view 230 mm, matrix 256 × 256, slice thickness 10 mm, voxel dimension 0.9 × 0.9 × 10.0 mm^3), Gaussian kernel 4 mm full width at half maxima (FWHM), height threshold (u) = 1.64, $p < 0.05$, (one-sided); finally overlaid onto the corresponding anatomical slice. On the right-hand side, the color-coded z-scale is given

Fig. 5 Continuous Performance Test (males, n = 12). Statistical parametric map of the z-scores. The display format is the averaged anatomical single slice with the orientation described above (n = 12). Data are presented for clusters and regions that survive the height and extent threshold detailed in Table 2. The color scale is arbitrary (*red scale*: positive activations; *blue scale*: negative activations)

the y-direction and 0.37° (SD: 0.12°) for rotation. The scans of all 12 study subjects showed a maximal translation < 2 mm and a rotation ≤ 2°. Cine check for postregistration residual motion and control for landmarks revealed highly accurate stereotaxis. The motion correction in both groups was comparable (Table 1).

Behavioural analysis (attentional performance)

The CPT-performance data for the study subjects were as follows: hit rate 0.90 (SD: 0.4), false-alarm rate 0.011 (SD: 0.014), response time 0.39 (SD: 0.08), d' 4.24 (SD: 0.99), lnβ 2.47 (SD: 1.38), omission errors 2.27 (SD: 4.59), and commission errors 1.44 (SD: 1.9). The probands in group A (n = 5) showed a perfect or nearly perfect performance, whereas subjects in group B (n = 7) were characterized by a poor, but not eccentric, performance profile.

Statistical maps

The results of the statistical analysis are summarized in Table 2.

Activations in a variety of cortical and subcortical regions were detected. A representative example is given in Fig. 4. In the overall group (n = 12; Fig. 5), activations in the right anterior cingulum, the dorsolateral prefrontal cortex, the superior temporal gyrus, the caudate nucleus and two thalamic nuclei (Ncl. dorsomedialis and anterior) were detected. Activation was strongly lateralized to the right hemisphere for both cortical and subcortical structures. The data in Table 2 are sorted with respect to the extent of activation and allow a comparison of the activated regions.

Areas of deactivation, i.e. regions with a negative correlation were detected in the posterior insular cortex, the adjacent structures of the superior temporal gyrus, in the region of the fusiform gyrus of both hemispheres and, to a lesser extent, in the left hippocampus and precentral region. These negative correlations generally did not reach the same size and spatial extent as the positive correlations.

The composite maps for each group and the difference image are given in Fig. 6. The good (n_A =5) and poor (n_B = 7) performers had a similar pattern of activation. In group A, the activation in the superior frontal gyrus, posterior insula and thalamus seems to be more symmetrical; activations of the anterior cingulum, mesial frontal lobe and nucleus caudatus were restricted to the right hemisphere. Areas of deactivation were localized in both the left and right posterior insular region, the superior colliculi, the left fusiform gyrus/hippocampus and, to a lesser extent, in the left cerebellum as well as the precentral and dorsolateral prefrontal cortex.

The low-performance group presented a similar activation pattern only for the anterior cingulum, thalamus and caudate nucleus. In contrast to the good performers, there was no significant activation in the mesial and lateral part of the superior frontal gyrus, but an extended activation in the right dorsolateral prefrontal cortex. Deactivation was observed in a small region of the right fusiform gyrus. The differences between both groups reached significance only for the right dorsolateral prefrontal cortex (see Fig. 6c).

Figure 7 gives the average signal response of the pixel of maximal activation and deactivation in a functionally defined region of interest (thalamus and left posterior in-

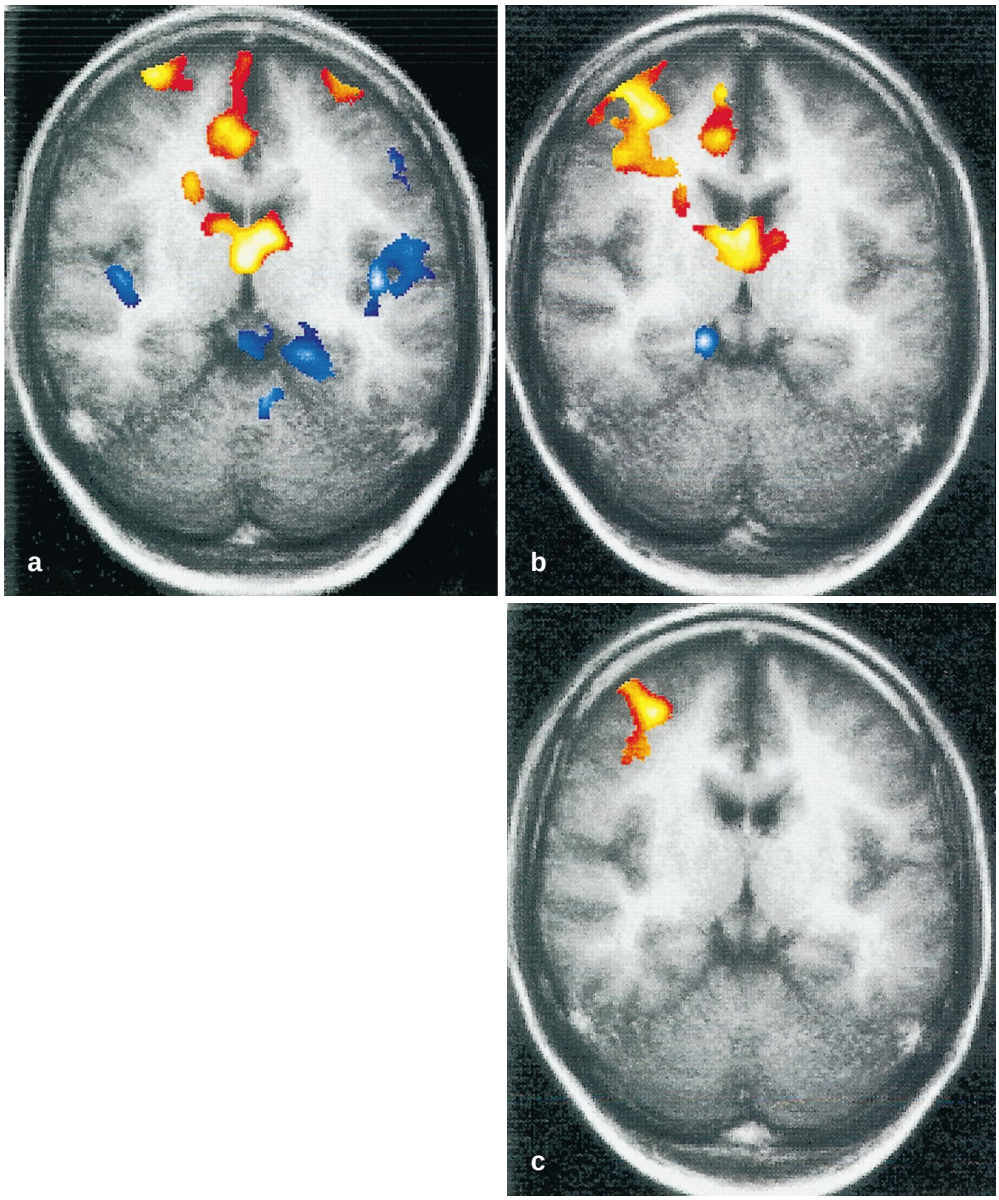

Fig. 6 a–c Continuous Performance Test (males, different levels of test performance). The display provides the SPM{Z} projected onto the averaged anatomical single slices with the orientation described herein ($n = 12$). Data are presented for clusters and regions that survive the height threshold for $p < 0.05$ and extent threshold for $p < 0.5$. The color scale is arbitrary (*red scale*: positive activations; *blue scale*: negative activations). **a** Group A (excellent performance); **b** group B (good performance); **c** significant differences between both groups (interaction group × condition; *blue scale*: group B > group A)

sula, respectively) of the total group, indicating a correlation of the signal course with the predefined stimulus function.

Discussion

The main findings of the present investigation are:

1. A right lateralized pattern of activation, not only cortically, but also in subcortical structures
2. Activation of an anatomical structure that up to now has not been described to be involved in attention processes: the right caudate nucleus
3. A divergent activation pattern for groups with different performance levels
4. Robust negative correlations (lowered pixel intensities) in the task condition as compared with the resting state, preliminarily named “deactivations”, in the region of the hippocampus and posterior insula.

With regard to item 1, almost all imaging studies using a CPT task as a cognitive challenge failed to report a distinctive lateralized response (Berman et al. 1986; Cohen and Servan-Schreiber 1994; Breiter 1995). Only Siegel et al. (1995) found that the CPT was associated with an increase in metabolic rate greatest in the right superior frontal gyrus. Our results are also in line with the findings of Van Horn et al. (1996) and Volz et al. (1997), who studied attentional processes in the frontal lobes by means of PET and fMRI using the Wisconsin Card Sorting Test (WCST). these authors also demonstrated a right lateralized activation in healthy probands. Van Horn et al. reported the right-sided lateralization effect only for the inferior part of the superior frontal gyrus, not for other frontal brain regions, suggesting that lateralized activation

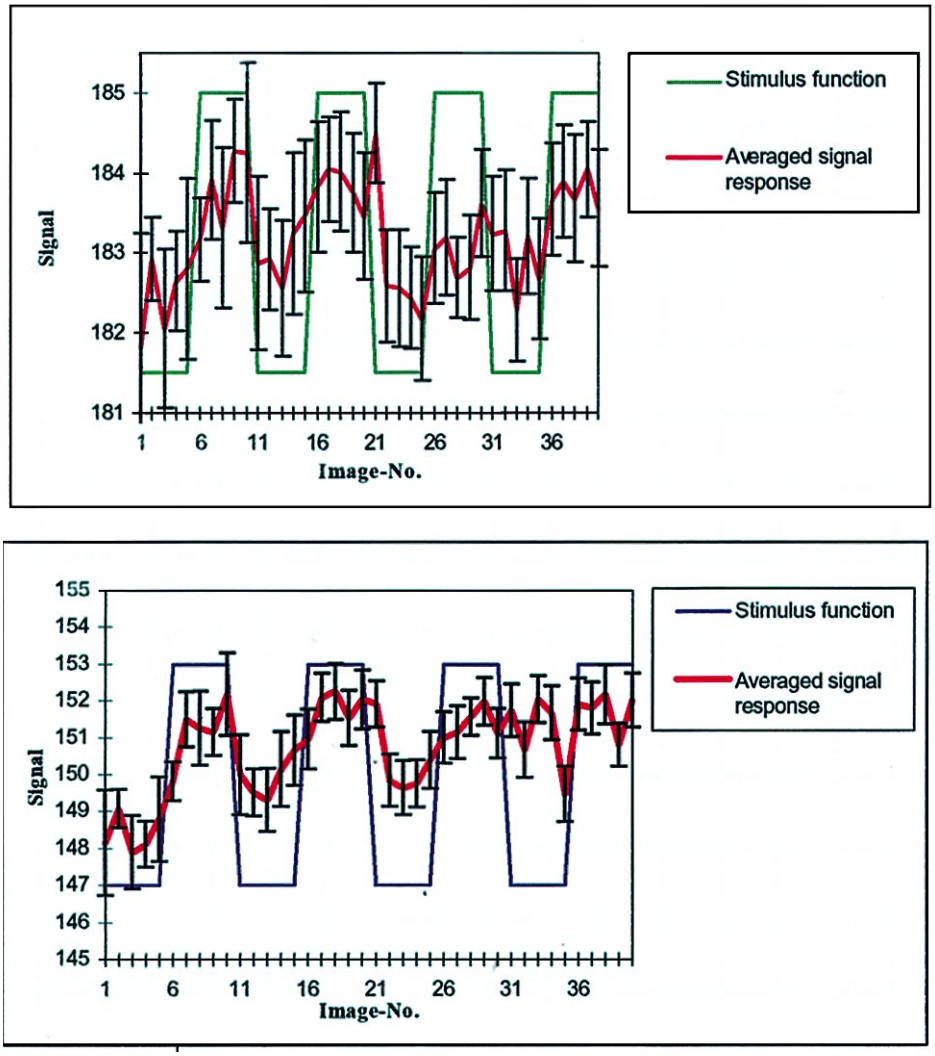

Fig. 7 a, b Averaged signal response (including standard deviations) of the voxels of maximal activation for the total group (n = 12). Positive activation: **a** right thalamus; **b** right gyrus cingulus anterior

might be confined to distinct brain regions. Together with the lateralized activation of the anterior cingulum found in PET studies (Petersen et al. 1989; Corbetta et al. 1991; Pardo et al. 1991; Heinze et al. 1994), our results corroborate the existence of right lateralized attentional networks as proposed by Posner et al. (1988), Posner and Petersen (1990) and Posner and Dehaene (1994). The inconsistent results for activation studies with respect to lateralization may be caused by failures to control for gender of the sample composition (Häger et al. 1996).

Subcortical structures, such as the thalamus and the basal ganglia, are involved in the modulation and maintenance of attention (Schneider 1984; Goldberg 1985; Buchsbaum and Haier 1987; LaBerge 1995). It is widely assumed that the thalamus plays a major role in attention (Heilman et al. 1994; LaBerge 1995). An attention-associated thalamic activation, which was predominant in the right hemisphere, was recently described in an fMRI study (Frith and Friston 1996). The authors related the activation to the nonspecific nuclei of the thalamus. The activation observed in the present investigation was localized in the mediodorsal and anterior nuclei of both hemispheres. These nuclei are relay stations for the dorsolateral prefrontal and anterior cingulate cortex. In a task requiring focal attention (Petersen et al. 1989), active areas were seen in the right anterior thalamus and caudate nucleus. In contrast to our findings, Siegel et al. (1995) reported a significantly increased metabolic rate in the left medial thalamus. In a study by Van Horn et al. (1996), thalamic activation seems more symmetrical, whereas Keilp et al. (1997) found a pattern of thalamic activation similar to our results in a more recent SPECT study for the CPT-number subtask.

The observed activation of the right caudate may demonstrate the output of the dorsolateral prefrontal cortex (DLPFC), which projects primarily to the caudate (Alexander et al. 1986).

With regard zu item 2, the activation of the right caudate nucleus, even reaching significance for both subgroups, has not yet been described in CPT activation studies. This result is not surprising, however, since the caudate receives the main output from the dorsolateral prefrontal cortex (Alexander et al. 1986). Recent PET studies (Petersen et al. 1989; Corbetta et al. 1991) found that the

caudate nucleus was activated in a focal and divided attention task. Van Horn et al. (1996) could also demonstrate a right-lateralized activation for the caudate.

With regard zu item 3, because of comparable β data for both groups, it is unlikely that performance differences are related to the level of effort or motivation. Our data suggest that performance seems negatively correlated with the extent of activation, at least for the dorsolateral prefrontal cortex. A possible interpretation might be that the more active region is less efficient and processes less data, although it consumes more energy, i.e. the more efficient the brain, the less energy it consumes (Haier et al. 1988; Fidelman 1994). The high-scoring subgroup showed a more symmetrical pattern of activations and deactivations. A tentative explanation might be that involvement of both frontal lobes makes task performance more effective because of improved bilateral information processing. Another important aspect of our data is the indication that in functional image analysis it is necessary to control for task-performance-related changes in the pattern of activation.

With regard zu item 4, inactive regions were projected symmetrically onto the left and right fusiform gyrus, the right parahippocampal/hippocampal and both posterior insular regions. The deactivation in the right pulvinar reaches significance only for the whole group.

Thus far, we cannot explain the mechanisms underlying the occurrence of negative correlations or *deactivations.* There is a small but growing body of literature dealing with the meaning of negative correlations in fMRI (Listerud et al. 1994; LeBihan and Dohi 1995; Lee et al. 1995; Lalonde 1996; McIntyre 1996; Popp 1996).

Possible explanations of such negative correlations might be lowered blood flow, inhibition due to higher cortical processing, or a local decoupling of oxygen consumption and blood flow changes. In the absence of changes in local blood flow, these decreases in signal may also reflect a local increase in the total amount of paramagnetic agents such as desoxyhaemoglobin, NO and oxygen.

There is some evidence for a localized decrease in metabolism and/or blood flow. Using a similar attentional paradigm as in the present study, Cohen et al. (1988) found a lowered metabolic rate in the anterior cingulum in a PET investigation; however, the investigated slices did not cover our region with negative correlations. In the recent PET study by Van Horn et al. (1996), regions with a significant lowered blood flow were the insular cortex and the anterior edge of the medial prefrontal cortex. Berman et al. (1995) observed in a recent PET study, with the WCST as a cognitive challenge, an activation in the DLPFC and a lowered blood flow in the left superior frontal and superior temporal gyrus. In contrast to PET, where deactivations are related to decreased blood flow or metabolism, the physiological mechanisms underlying these effects in fMRI are far from being understood. The results have to be interpreted very cautiously and depend strongly on the resting condition. Some authors even argue that all these results are due to artefacts. We assume that artificial genesis of the observed deactivations is not probable, since they are very robust, and therefore merit further research.

It remains possible, however, that our findings resulted from the intrinsic restrictions of our fMRI method. First of all, the lack of symmetrical activation findings might be a function of limited statistical power. There is another explanation for the obviously different activation pattern in the studies cited above. Although similar, the versions of the CPT may differ with regard to the amount of attention they require. It was recently shown that only subtle alterations in stimulus parameters can invert the lateralization pattern of the CPT (Keilp et al. 1997). Contrasting the CPT-double or CPT-IP in our CPT-double/T- task elements of context did not change from trial to trial. Compared with experiments with the CPT-double/-IP task (Cornblatt et al. 1988; Cornblatt et al. 1989) the CPT-double/T- task used in our experiment demands less internal representation of context.

On the other hand, the CPT-double/T is more demanding than the CPT-X or CPT-number subtask, where the target event is the appearance of a single stimulus (Buchsbaum et al. 1990; Schroeder et al. 1994; Siegel et al. 1995; Keilp et al. 1997). A direct comparison with other studies seems difficult, because the template used does not cover all the regions of interest investigated by the other groups. This is a problem especially in the case of the two fMRI studies using an attentional paradigm (Cohen and Servan-Schreiber 1994; Breiter 1995). The source of the fMRI signal is still a controversial subject; therefore, it is problematic to compare fMRI and PET/SPECT studies directly.

Taken together, our data indicate that in males the right anterior cingulate and dorsolateral prefrontal cortex are parts of an attentional system, similar to the anterior attention system of Posner and Petersen (1990) and Posner and Raichle (1995). Posner (1994) characterized the sequence of elementary mental operations assessed by the visual attentional network as disengaging from the current focus of attention, shifting attention to the cued localization, and amplifying the target. He proposed that the subsystem responsible for alerting/vigilance is located in the right anterior hemisphere. Because two of the putative three attentional circuits could be located in the right hemisphere, it seems reasonable to interpret our data as a confirmation of the right-lateralized anterior attentional network. These results are supported by lesion studies, suggesting that damage to the right hemisphere is more often associated with elements of the neglect syndrome.

Despite the inherent pitfalls of the single-slice technique, representative functional images of important parts of the anterior attention system were obtained. At least in males, this function seems to be lateralized to the right hemisphere. Thus, our findings may provide a deeper understanding of the neural networks underlying hemispheric mechanisms.

Acknowledgement This work was supported by a grant of BMBF (01 ZZ 9602).

References

Alexander GE, DeLong MR, Strick PL (1986) Parallel organization of functionally segregated circuits linking basal ganglia and cortex. Annu Rev Neurosci 9: 357–381

Berman KF, Zec RF, Weinberger DR (1986) Physiologic dysfunction of dorsolateral prefrontal cortex in schizophrenia. II. Role of neuroleptic treatment, attention, and mental effort (see comments). Arch Gen Psychiatry 43: 126–135

Breiter HC (1995) FMRI of effortful attention using Talairach averaging across subjects. Third Meeting of the SMR 2, p 1348

Buchsbaum MS, Haier RJ (1987) Functional and anatomical brain imaging: impact on schizophrenia research. Schizophr Bull 13: 115–132

Buchsbaum MS, Nuechterlein KH, Haier RJ, Wu J, Sicotte N, Hazlett E, Asarnow R, Potkin S, Guich S (1990) Glucose metabolic rate in normals and schizophrenics during the Continuous Performance Test assessed by positron emission tomography. Br J Psychiatry 156: 216–227

Buchsbaum MS, Haier RJ, Potkin SG, Nuechterlein K, Bracha HS, Katz M, Lohr J, Wu J, Lottenberg S, Jerabek PA, Bunney W (1992) Frontostriatal disorder of cerebral metabolism in never-medicated schizophrenics. Arch Gen Psychiatry 49: 935–942

Cohen JD, Servan-Schreiber D (1994) Activation of the prefrontal cortex in a nonspatial working memory task with FMRI. Hum Brain Mapping 1: 293–304

Cohen RM, Semple WE, Gross M, Nordahl TE, DeLisi LE, Holcomb HH, King AC, Morihisa JM, Pickar D (1987) Dysfunction in a prefrontal substrate of sustained attention in schizophrenia. Life Sci 40: 2031–2039

Cohen RM, William WE, Gross M, Holcomb HH, Dowling MS, Nordahl TE (1988) Functional localization of sustained attention: comparison to sensory stimulation in the absence of instruction. Neuropsychiatry Neuropsychol Behav Neurol 1: 3–20

Corbetta M, Miezin FM, Dobmeyer S, Shulman GL, Petersen SE (1991) Selective and divided attention during visual discriminations of shape, color, and speed: functional anatomy by positron emission tomography. J Neurosci 11: 2383–2402

Cornblatt BA, Risch NJ, Faris G, Friedman D, Erlenmeyer Kimling L (1988) The Continuous Performance Test, identical pairs version (CPT-IP). I. New findings about sustained attention in normal families. Psychiatry Res 26: 223–238

Cornblatt BA, Lenzenweger MF, Erlenmeyer Kimling L (1989) The continuous performance test, identical pairs version. II. Contrasting attentional profiles in schizophrenic and depressed patients. Psychiatry Res 29: 65–85

Egan JP (1980) Signal detection theory and ROC analysis. Academic Press, New York

Fidelman U (1994) A misleading implication of the metabolism scans of the brain. Int J Neurosci 74: 105–108

Friston K (1996) Statistic parametric mapping. Wellcome Department of Cognitive Neurology

Friston KJ, Holmes A, Poline JB, Price CJ, Frith CD (1996) Detecting activations in PET and fMRI: levels of inference and power. Neuroimage 4: 223–235

Frith CD, Friston KJ (1996) The role of the thalamus in "top down" modulation of attention to sound. Neuroimage 4: 210–215

Goldberg E (1985) Akinesia, tardive dysmentia and frontal lobe disorders in schizophrenia. Schizophr Bull 11: 255–263

Grier JB (1971) Nonparametric indexes for sensitivity and bias: computing formulas. Psychol Bull 79: 424

Häger F, Volz HP, Gaser C, Mentzel HJ, Kaiser WA, Sauer H (1996) Gender differences revealed by functional fMRI during the continuous performance test in the frontal cortex. Neuroimage 3: 182

Haier RJ, Siegel B, Nuechterlein KH, Hazlett E, Buchsbaum MS (1988) Cortical glucose metabolic rate correlates of abstract reasoning and attention studied with PET. Intelligence 12: 199–217

Heilman KM, Watson RT, Valenstein E (1994) Localization of lesions in neglect and related disorders. In: Kertesz A (ed) Localization and neuroimaging in neuropsychology. Academic Press, San Diego, pp 495–524

Heinze HJ, Mangun GR, Burchert W, Hinrichs H, Scholz M, Münte TF, Gös A, Scherg M, Johannes S, Hundeshagen H, Gazzaniga MS, Hillyard SA (1994) Combined spatial and temporal imaging of brain activity during visual selective attention in humans. Nature 372: 543–546

Keilp JG, Herrera J, Stritzke P, Cornblatt BA (1997) The continuous performance test, identical pairs version (CPT-IP): brain functioning during performance of numbers and shapes subtask. Psychiatry Res Neuroimaging 74: 35–45

LaBerge D (1995) Attentional processing. Harvard University Press, Cambridge, Mass

Lalonde FM, Jezzard P, Weisberg JA (1996) A difference in fMRI time course between areas of increased and decreased neural activity. Neuroimage 3:74

LeBihan D, Dohi M (1995) Can fMRI detect decreased neuronal activity? Proc 3rd SMR 1, p 452

Lee AT, Glover GH, Meyer CH (1995) Discrimination of large venous vessels in time-course spiral blood-oxygen-level-dependent magnetic-resonance functional neuroimaging. Magn Reson Med 33: 745–754

Listerud J, Lopez-Villegas L, Isaac G, Detre J (1994) Validation of regions of positive and negative correlation to stimulus observed on students t maps calculated from functional MRI studies in normal volunteers. Proc 3rd SMR 2, p 634

McIntyre MC, Wennerberg A, Somorjai R, et al. (1996) Activation and deactivation in functional brain images. Neuroimage 3: 82

Mirsky AF, Anthony BJ, Duncan CC, Ahearn MB, Kellam SG (1991) Analysis of the elements of attention: a neuropsychological approach. Neuropsychol Rev 2: 109–145

Nestor PG, Faux SF, McCarley RW, Sands SF, Horvath TB, Peterson A (1991) Neuroleptics improve sustained attention in schizophrenia. A study using signal detection theory. Neuropsychopharmacology 4: 145–149

Neuroscan (1990) STIM. VISCPT. Neurosoft Inc.

Nuechterlein KE (1991) Vigilance in schizophrenia and related disorders. In: Steinhauer SR, Gruzelier JH, Zubin J (eds) Handbook of schizophrenia, vol 5. Elsevier, Amsterdam, pp 397–433

Pardo JV, Fox PT, Raichle ME (1991) Localization of a human system for sustained attention by positron emission tomography. Nature 349: 61–64

Petersen SE, Corbetta M, Miezin FM, Dobmeyer SM (1989) Selective attention modulates visual processing of form, color and velocity. III. Areas related to higher order selective processes. J Neurosci 15: 624

Pollack I, Norman DA (1964) A non-parametric analysis of recognition experiments. Psychonom Sci 1: 125

Popp CA, Trudeau JD, Biswal B (1996) Negative pixels in functional maps of sensorimotor tasks. Neuroimage 3:165

Posner MI, Dehaene S (1994) Attentional networks. Trends Neurosci 17: 75–79

Posner MI, Petersen SE (1990) The attention system of the human brain. Annu Rev Neurosci 13: 25–42

Posner MI, Raichle ME (1995) Precis of images of mind. Behav Brain Sci 18: 327–383

Posner MI, Petersen SE, Fox PT, Raichle ME (1988) Localization of cognitive operations in the human brain. Science 240: 1627–1631

Pugh KR, Shaywitz BA, Shaywitz SE, Fulbright RK, Byrd D, Skudlarski P, Shankweiler DP, Katz L, Todd Constable T, Fletcher J, Lacadie C, Marchione K, Gore JC (1996) Auditory selective attention: an fMRI investigation. Neuroimage 4: 159–173

Rezai K, Andreasen NC, Alliger R, Cohen G, Swayze VD, O'Leary DS (1993) The neuropsychology of the prefrontal cortex. Arch Neurol 50: 636–642

Rosvold HE, Mirsky A, Sarason I, Bransome ED, Beck LH (1956) A continuous performance test of brain damage. J Consult Psychol 20: 343–350

Schneider JS (1984) Basal ganglia role in behavior: importance of sensory gating and its relevance to psychiatry. Biol Psychiatry 19: 1693–1710

Schroeder J, Buchsbaum MS, Siegel BV, Geider FJ, Haier RJ, Lohr J, Wu J, Potkin SG (1994) Patterns of cortical activity in schizophrenia. Psychol Med 24: 947–955

Siegel BV Jr, Asarnow R, Tanguay P, Call JD, Abel L, Ho A, Lott I, Buchsbaum MS (1992) Regional cerebral glucose metabolism and attention in adults with a history of childhood autism. J Neuropsychiatry Clin Neurosci 4: 406–414

Siegel BV Jr, Buchsbaum MS, Bunney WE Jr, Gottschalk LA, Haier RJ, Lohr JB, Lottenberg S, Najafi A, Nuechterlein KH, Potkin SG, et al. (1993) Cortical–striatal–thalamic circuits and brain glucose metabolic activity in 70 unmedicated male schizophrenic patients. Am J Psychiatry 150: 1325–1336

Siegel BV, Nuechterlein KH, Haier RJ, Wu J, Sicotte N, Hazlett E, Asarnow R, Potkin S, Guich S (1995) Glucose metabolic correlates of continuous performance test performance in adults with a history of infantile autism, schizophrenics, and controls. Schizophr Res 17: 85–94

Talairach J, Tournoux P (1988) Co-planar stereotaxic atlas of the human brain. Thieme, Stuttgart

Van Horn JD, Berman KF, Weinberger DR (1996) Functional lateralization of the prefrontal cortex during traditional frontal lobe tasks. Biol Psychiatry 39: 389–399

Volz H, Gaser C, Häger F, Rzanny R, Mentzel HJ, Kreitschmann-Andermahr I, Kaiser WA, Sauer H (1997) Brain activation during cognitive stimulation with the Wisconsin Card Sorting Test: a functional MRI study on healthy volunteers and on schizophrenics. Psychiatry Res Neuroimaging 75: 145–157

Weintraub S, Mesulam MM (1985) Mental state assessment of young and elderly adults in behavioral neurology. In: Mesulam MM (ed) Principles of behavioral neurology. Davies, Philadelphia, pp 71–123